Noncubic symmetry in Ca 1 − x Eu x B 6 (0.15 ≤ x 1.00) : An electron-spin-resonance study

R. R. Urbano, P. G. Pagliuso, C. Rettori, P. Schlottmann, Z. Fisk, and S. B. Oseroff

---

Articles you may be interested in

Broadband electron spin resonance in a nanosized La0.25Ca0.75MnO3 manganite
J. Appl. Phys. **116**, 053909 (2014); 10.1063/1.4892443

Structure and dynamics of S 3 − radicals in ultramarine-type pigment based on zeolite A: Electron spin resonance and electron spin echo studies
J. Chem. Phys. **130**, 204504 (2009); 10.1063/1.3124551

Electron spin resonance studies of Bi 0.55 Ca 0.45 MnO 3 nanoparticles
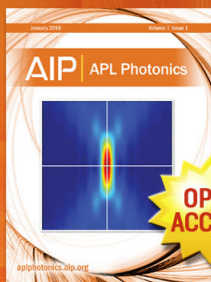J. Appl. Phys. **105**, 07D718 (2009); 10.1063/1.3075988

Electron-spin-resonance study of gadolinium borosilicide: A rare-earth ladder compound
J. Appl. Phys. **99**, 08J309 (2006); 10.1063/1.2169471

Magnetic frustration in Y-doped manganites: Electron spin resonance and magnetization
J. Appl. Phys. **87**, 5603 (2000); 10.1063/1.372464

Noncubic symmetry in $Ca_{1-x}Eu_xB_6$ ($0.15 \lesssim x \le 1.00$): An electron-spin-resonance study

R. R. Urbano, P. G. Pagliuso, and C. Rettori[a]
Instituto de Física "Gleb Wataghin," UNICAMP, 13083-970 Campinas, Sao Paulo, Brazil

P. Schlottmann
Department of Physics, Florida State University, Tallahassee, Florida 32306
and National High Magnetic Field Laboratory, Florida State University, Tallahassee, Florida 32306

Z. Fisk
Department of Physics, University of California at Davis, Davis, California 95616

S. B. Oseroff
San Diego State University, San Diego, California 92182

(Presented on 2 November 2005; published online 18 April 2006)

The Eu^{2+} ($4f^7$, $S=7/2$) g value in $Ca_{1-x}Eu_xB_6$ ($0.15 \lesssim x \le 1.00$) was measured by means of electron spin resonance at two frequencies (fields), 9.4 (≈ 3.4 kOe) and 34.4 GHz (≈ 12.1 kOe). The g value was found to be anisotropic and magnetic-field dependent. The amplitude of the anisotropy increases at low temperatures. The observed angular and temperature dependences of the g value suggest tetragonal symmetry caused, presumably, by a distortion along a direction perpendicular to the largest crystal face, the [001] direction. Due to the platelet shape of the samples, part of the anisotropy of the g value can also be attributed to demagnetization effects. The g values decrease at higher fields, which is interpreted in terms of a two-band model involving an exchange interaction between the localized Eu^{2+} $4f^7$ electrons with conduction Eu^{2+} $5d$-like electrons and B $2p$-like holes. © *2006 American Institute of Physics.* [DOI: 10.1063/1.2164427]

Over the past decades the cubic hexaboride compounds RB_6 ($R=$rare/alkaline earths, space group 221, $Pm3m$) have been the subject of intensive studies, both experimental and theoretical, due to their variety of exotic effects and interesting physical properties such as ferromagnetism, weak ferromagnetism, metal-insulator transition, large negative magnetoresistance, quadrupolar ordering, Jahn-Teller effect, superconductivity, heavy fermion, fluctuating valence, and Kondo lattice behaviors.[1–13] Among them the semimetal EuB_6 is particularly interesting because of the formation of magnetic polarons, changing the magnetic and transport properties, and the two transitions observed at $T_{c1}=15.3$ K and $T_{c2}=12.7$ K.[4,6,14] The one at T_{c1} is believed to correspond to the percolation transition of the polarons and is accompanied by a semimetal to metal transition, while below T_{c2} all Eu^{2+} spins participate in the ferromagnetic (FM) long-range order.

In previous reports[15,16] we have studied the evolution from insulator ($x=0$) to semimetal ($x=1.00$) in $Ca_{1-x}Eu_xB_6$ by measuring the Eu^{2+} ($4f^7$, $S=7/2$) electron-spin-resonance (ESR) linewidth (ΔH). Due to the broken translational invariance in an alloy, each Eu^{2+} ion introduces a bound state in the gap of the insulator CaB_6. Our results indicate that at $x \approx 0.15$ the bound states percolate leading to a metallic environment with a spin-flip relaxation process involving magnetic polarons and the symmetry of the Fermi surface. $x \approx 0.15$ corresponds to the site percolation of random nearest- and next-to-nearest-neighbor bonds. Note that the next-to-next-to-nearest-neighbor bonds ([111] direction) are blocked for the propagation of the wave functions by the large B_6 anions.

In the present work we report on the field dependence of the Eu^{2+} ($4f^7$, $S=7/2$) ESR g shift and its angular dependence. We explain the field dependence of the g shift in terms of the exchange interaction between the localized Eu^{2+} $4f^7$ electrons with the conduction Eu^{2+} $5d$-like electrons and B_6^{2-} $2p$-like holes. We attribute the angular dependence of the g value and its T dependence to a tetragonal distortion along the directions perpendicular to the (001) natural growth faces of the crystal. The distortion is believed to arise from the surface of the crystal and propagates deep into the crystal. This effect, which is present only in the metallic phase, is enhanced by the crystalline field splitting of the $5d$ electrons at low temperatures. Due to the platelet shape of the samples, part of the anisotropy of the g value can also be attributed to demagnetization effects.

Platelet ($\sim 1.2 \times 0.9 \times 0.2$ mm^3) single crystals of $Ca_{1-x}Eu_xB_6$ ($0.003 \lesssim x \le 1.00$) were grown, as described in Ref. 2. The structure and phase purity were checked by x-ray powder diffraction and the crystal orientation determined by Laue x-ray diffraction. The faces of natural growth of the crystals are called (001) planes and are relevant to the g value anisotropy investigation. The ESR experiments were performed in a Bruker spectrometer using an X-band (9.48 GHz) TE_{102} room-T cavity and a Q-band (34.48 GHz) cool split-ring cavity, both coupled to a T controller using a helium gas flux system for $4.2 \lesssim T \le 300$ K. The ESR spectra were analyzed in terms of Dyson's theory for the resonance
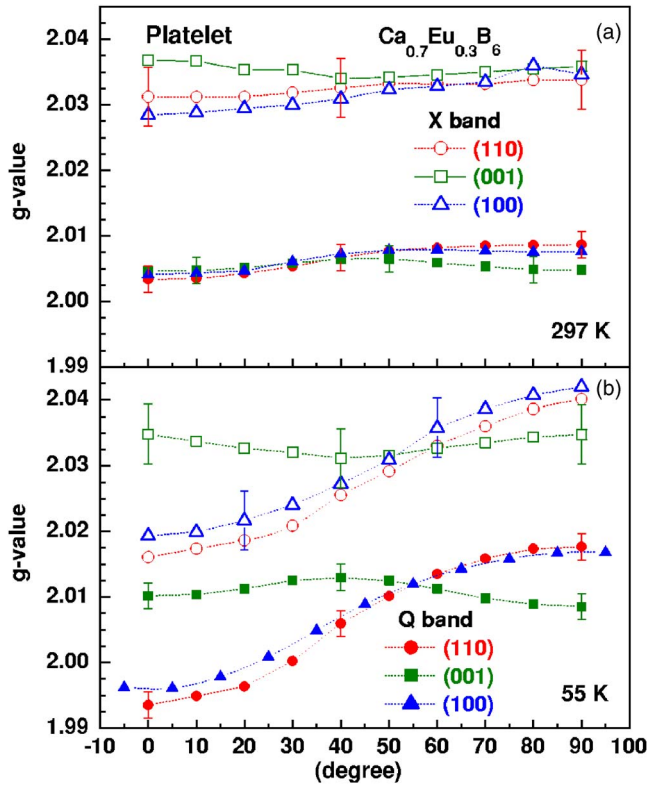
[a] Electronic mail: rettori@ifi.unicamp.br

FIG. 1. (Color online) Angular dependence of the *X*- and *Q*-band ESR *g* values for Eu^{2+} in a Ca$_{1-x}$Eu$_x$B$_6$ plateletlike single crystal for *x*=0.30 at (a) room *T* and (b) 55 K. The magnetic field *H* was rotated in the (001), (110), and (100) planes. θ=0 corresponds to *H*∥[001]. The dashed lines are guide for the eye.

FIG. 2. (Color online) Angular dependence of the *X*- and *Q*-band ESR *g* values for Eu^{2+} in a EuB$_6$ plateletlike single crystal at (a) room *T* and (b) 55 K. The magnetic field *H* was rotated in the (001), (110), and (100) planes. θ=0 corresponds to *H*∥[001]. The dashed lines are guide for the eye.

line shape.[17] In the pertinent range of *T*, the resistivity of our crystals changes from ~0.5 to ~5 mΩ cm, which corresponds to microwave (*X* and *Q* bands) penetration skin depths of about 5–25 μm. $M(T,H)$ measurements for $2 \lesssim T \lesssim 300$ K were taken in a Quantum Design superconducting quantum interference device-reciprocating sample option (SQUID-RSO) dc magnetometer. The Eu^{2+} concentration in our crystals was determined from Curie-Weiss fits to the susceptibility data. The experimental data presented in this work were obtained on the same samples used in our previous work.[15,16] The high quality of the crystals was determined by magnetoresistance and heat-capacity measurements.[15,16]

Figures 1 and 2 present the angular dependence of the *g* value for the plateletlike crystals measured at the *X* and *Q* bands in the (110), (100), and (001) planes at ~297 and ~55 K for *x*=0.30 and *x*=1.00, respectively. Similar results were obtained for the *x*=0.60 crystal (not shown here). The (001) plane coincides with the largest crystal face. The data show the following features: (i) The angular dependence of the *g* value displays a surprising tetragonal symmetry with the twofold axis being perpendicular to the largest crystal face,[18] in spite of the overall cubic symmetry found for the anisotropy of the linewidth (see Figs. 6 and 7 in Ref. 16); (ii) the amplitude of the *g* value anisotropy, $g_\perp - g_\parallel$, is nearly *H* and *x* independent; (iii) this amplitude increases at low *T*; and (iv) the *g* value decreases with *H*.

The reduction in the positive *g* shift ($\Delta g = g - 1.988$) at high fields (see *Q*-band data in Figs. 1 and 2) may be under-
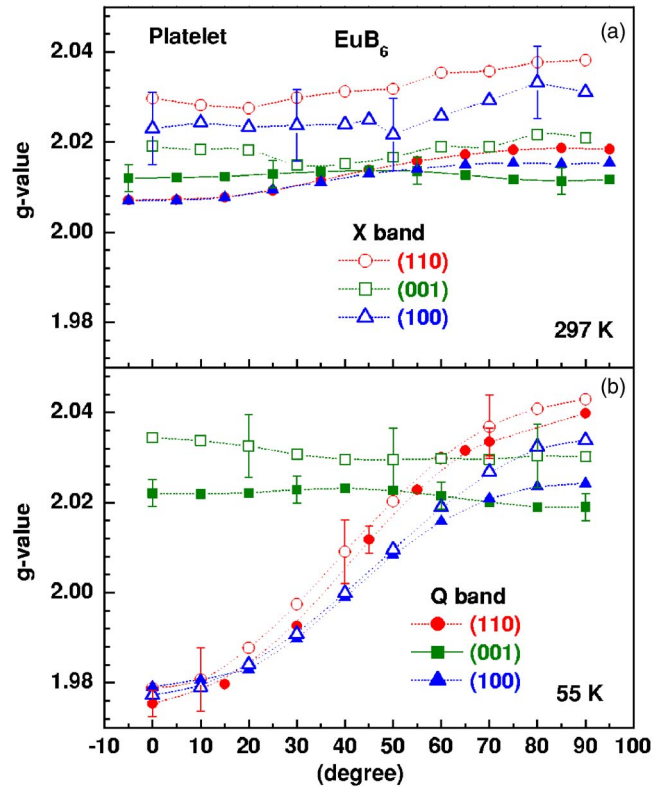
stood in terms of a two-band model[19,20] involving the exchange interaction between the localized Eu^{2+} 4f^7 electrons with (i) the conduction Eu^{2+} 5d-like electrons and (ii) the B 2p-like holes.[21] The exchange interaction with the 5d-like electrons is assumed to be of atomic type, $J_{at}^e > 0$, and that with the B 2p-like holes of covalent origin, $J_{cv}^h < 0$. The magnitudes of the exchange constants have been estimated in Ref. 21 to be $|J_{at}^e| \approx 100$ meV and $|J_{cv}^h| \approx 5$ meV. The latter is expected to be small because of the almost ionic bond nature of the crystal. Thus, the *g* shift can be written as $\Delta g = \Delta g_e + \Delta g_h = [J_{at}^e(0)\langle s_z^e \rangle + J_{cv}^h(0)\langle s_z^h \rangle]/(\mu_B H)$, where $J_{at}^e(0)$ and $J_{cv}^h(0)$ are the $q=0$ component (zero-momentum transfer between electrons),[22] and $\langle s_z^e \rangle$ and $\langle s_z^h \rangle$ are the spin polarizations of the electrons and holes, respectively. The semimetal is not compensated, since it contains more electrons in the conduction band than holes in the valence band (B$_6$ deficiency). Since $|J_{at}^e| \gg |J_{cv}^h|$, the *g* shift is dominated by the electrons and necessarily positive. For low fields the *g* shift is then given by $\Delta g/g = J_{at}^e(0) \eta_F^e + J_{cv}^h(0) \eta_F^h$, where η_F^e and η_F^h are the carrier densities of electrons and holes at the Fermi level, respectively. As the field increases, the atomiclike 5d-electrons spin polarize and $\Delta g \approx J_{at}^e(0)\langle s_z^e \rangle/(\mu_B H)$ decreases with *H*, as observed in Figs. 1 and 2.

The unexpected tetragonal symmetry revealed by the angular dependence of the *g* value, shown in Figs. 1 and 2 for $x \gtrsim 0.30$, is *H* and *x* independent within the accuracy of our experiments. The data were also taken at $T \gg T_{c1}$, i.e., at temperatures where the magnetic short-range order is small. Since the ESR signal in plateletlike crystals mainly arises

from the Eu^{2+} ions within the microwave skin depth of the two largest crystal faces, the g value anisotropy must be caused by a tetragonal distortion within the microwave skin depth of the crystal with the fourfold symmetry axis along the [001] direction (see Figs. 1 and 2). A strong demagnetization due to the platelet shape of the sample would give rise to a similar effect.

Moreover, since the g value anisotropy is almost the same for X and Q bands, the distortion should be nearly uniform over a distance of the order of the the skin depth of the corresponding microwaves. Thus, the distortion, presumably arising at the surface, must penetrate deeply into the crystal. The amplitude of the g value angular dependence also increases at lower T, which is consistent with an increasing distortion as T is lowered.

A possible explanation of this symmetry reducing distortion of the lattice is the following. The binding energy of the crystal is predominantly ionic and given by the Madelung sum of the Coulomb interaction between all the ions. For the bulk, choosing a Eu^{2+} as the origin, this sum can be viewed as a sum over shells of equidistant (measured from the origin) ions. These shells have alternating charges, thus leading to effective (radial) dipolar contributions. Since the Coulomb interaction falls off only as the inverse of the distance, a very large number of shell pairs will contribute to the binding energy. At a distance z from the surface of the crystal only spherical shells of radius less than z are complete. Shells of radius larger than z are incomplete in the direction of the surface. Hence, the dipoles contributing to the binding energy at distances larger than z in the direction of the surface are missing. This imbalance introduces an axial symmetry and has as a consequence, an elongation of the lattice spacing in the [001] direction. Hence, the crystal has effectively a tetragonal symmetry with [001] being the fourfold axis. This distortion affects the crystalline splitting of the $5d$ electrons and via the exchange J_{at}^{e} induces a g value anisotropy of Eu^{2+} in the metallic phase. Since the carrier density increases as T is lowered, the anisotropy should increase with decreasing T.

In summary, we have reported the field, angular, and temperature dependences of the g value in the ESR of $Ca_{1-x}Eu_xB_6$ for $0.30 \lesssim x \leq 1.00$. The observed field-reduced g shift was interpreted in terms of an exchange interaction between the localized Eu^{2+} $4f^7$ electrons with two types of conduction electrons (two-band model), Eu^{2+} $5d$-like electrons and B $2p$-like holes. The tetragonal angular dependence of the g value and its temperature dependence were associated with a crystal distortion within (or beyond) the

microwave skin depth, with the tetragonal axis perpendicular to the crystal (001) faces. It should be stressed that the anisotropy of the g value appears to be at variance with x-ray and neutron-scattering measurements, where a departure from cubic symmetry was not observed. However, a small lattice distortion amplified by the $5d$-electron crystalline field could lead to an effect measurable by ESR but too small to be detected by x rays and neutrons.[7] Demagnetization effects due to the shape of the sample can also contribute to the anisotropy of the g value.

[1]J. Etourneau and P. Hagenmuller, Philos. Mag. B **52**, 589 (1985).
[2]D. P. Young *et al.*, Nature (London) **397**, 412 (1999).
[3]M. E. Zhitomirsky, T. M. Rice, and V. I. Anisimov, Nature (London) **402**, 251 (1999).
[4]L. Degiorgi, E. Felder, H. R. Ott, J. L. Sarrao, and Z. Fisk, Phys. Rev. Lett. **79**, 5134 (1997).
[5]S. Massidda, A. Continenza, T. M. de Pascale, and R. Monnier, Z. Phys. B: Condens. Matter **102**, 83 (1997).
[6]S. Süllow *et al.*, Phys. Rev. B **57**, 5860 (1998).
[7]C. H. Booth, J. L. Sarrao, M. F. Hundley, A. L. Cornelius, G. H. Kwei, A. Bianchi, Z. Fisk, and J. M. Lawrence, Phys. Rev. B **63**, 224302 (2001).
[8]S. Paschen, D. Pushim, M. Schlatter, P. Vonlanthen, H. R. Ott, D. P. Young, and Z. Fisk, Phys. Rev. B **61**, 4174 (2000).
[9]G. A. Wigger, Ch. Walti, H. R. Ott, A. D. Bianchi, and Z. Fisk, Phys. Rev. B **66**, 212410 (2002).
[10]G. A. Wigger, C. Beeli, E. Felder, H. R. Ott, A. D. Bianchi, and Z. Fisk, Phys. Rev. Lett. **93**, 147203 (2004).
[11]G. Uimin, Phys. Rev. B **55**, 8267 (1997).
[12]H. Sturm, B. Elschner, and K.-H. Hock, Phys. Rev. Lett. **54**, 1291 (1985).
[13]T. S. Altshuler and M. S. Bresler, J. Exp. Theor. Phys. **88**, 1019 (1999).
[14]S. Süllow, I. Prasad, M. C. Aronson, S. Bogdanovich, J. L. Sarrao, and Z. Fisk, Phys. Rev. B **62**, 11626 (2000).
[15]R. R. Urbano, P. G. Pagliuso, C. Rettori, S. B. Oseroff, J. L. Sarrao, P. Schlottmann, and Z. Fisk, Phys. Rev. B **70**, 140401 (2004).
[16]R. R. Urbano *et al.*, Phys. Rev. B **71**, 184422 (2005).
[17]G. Feher and A. F. Kip, Phys. Rev. **98**, 337 (1955); F. J. Dyson, *ibid.* **98**, 349 (1955); G. E. Pake and E. M. Purcell, *ibid.* **74**, 1184 (1948).
[18]A. Abragam and B. Bleaney, *EPR of Transition Ions* (Clarendon, Oxford, 1970).
[19]S. Kunii, T. Uemura, Y. Chiba, T. Kasuya, and M. Date, J. Magn. Magn. Mater. **52**, 271 (1985); S. Kunii, J. Phys. Soc. Jpn. **69**, 3789 (2000).
[20]P. M. Bisch, A. Troper, and A. A. Gomes, Phys. Rev. B **13**, 3902 (1976); A. Troper, O. L. T. de Menezes, P. Lederer, and A. A. Gomes, *ibid.* **18**, 3709 (1978); G. E. Barberis, D. Davidov, J. P. Donoso, C. Rettori, J. F. Suassuna and H. D. Dokter, Phys. Rev. B **19**, 5495 (1979); P. G. Pagliuso, C. Rettori, J. L. Sarrao, A. Cornelius, M. F. Hundley, Z. Fisk, and S. B. Oseroff, *ibid.* **60**, 13515 (1999).
[21]M. J. Calderón, L. G. L. Wegener, and P. B. Littlewood, Phys. Rev. B **70**, 092404 (2004).
[22]D. Davidov, K. Maki, R. Orbach, C. Rettori, and E. P. Chock, Solid State Commun. **12**, 621 (1973).